# ANALYSIS OF CRYSTAL STRUCTURE AND TEXTURE ON AL-5052 ROD PROCESSED BY ECAP AND POST-ECAP ANNEALING AT 100-300 °C

**Ibrahim Purawiardi[1],\* and I Nyoman Gede Putrayasa Astawa[1]**
[1]Research Centre for Metallurgy and Materials, Indonesian Institute of Sciences (LIPI),
National Science and Technology Park (PUSPIPTEK) Bld. 470, South Tangerang 15314, Banten

\*E-mail: ibrahimpurawiardi@gmail.com

## ABSTRACT

*Equal-channel angular pressing (ECAP) treatment is a method to improve mechanical properties of bulk metals without adding or extracting their alloy elements. The ECAP process can improve severe plastic deformation that will increase mechanical properties such as hardness and modulus of elasticity. The disadvantage of ECAP product is non-uniform mechanical properties. To solve this problem, post-ECAP annealing process can be applied in order to form more uniform mechanical properties. This phenomena should also be caused by the change of crystal structure and texture during this process. However, study of the change of crystal structure and texture during ECAP and followed by annealing process was seldom done. This study aims to try to determine the characteristics of crystal structure and texture of ECAPed and post-ECAP-annealed materials with annealing temperature variation of 0, 100, 200 and 300 °C. Four Al-5052 alloy rods were used as material samples. The results of this study show that annealing process can homogenize the crystal structure of ECAPed Al-5052 rod. On the other hands, the texture characteristics of ECAPed Al-5052 rod becomes more random as an implication of increasing of annealing temperature.*

*Keywords: ECAP; Al-5052; annealing; crystal structure; texture.*

## 1. INTRODUCTION

Al-5052 alloy is a material that is widely used in marine and chemical-based industries due to a combination of corrosion resistance and mechanical properties such as tensile strength, toughness, fatigue resistance and fracture resistance [1,2]. In addition, Al-5052 alloys have also begun to be widely used in the automotive industry because of their light weight [3].

Several ways have been done to create the ultrafine grain (UFG) structure to improve the mechanical properties of Al-5052 alloys through plastic deformation methods such as ECAP, accumulative roll bonding and high-pressure torsion [4]. Among the plastic deformation methods, the ECAP method is a method that can be applied to Al-5052 rod. The ECAP mechanism itself is forcibly pushing solid rod samples with a certain load so that they pass through a cylindrical channel with a certain angular turn on a dies [5]. In addition to theoretically being able to produce structures with homogeneous grain size [6], the ECAP process in solid rods has also been shown to improve its mechanical properties such as improving hardness and tensile strength, and reducing the strain value [7,8].

However, in practice, it turns out that not all results of ECAP treatment on Al-5052 rods can produce structures with homogeneous grain sizes [9]. It can occur if the ECAP treatment on Al-5052 rod is carried out at room temperature [9]. However, this condition can still be improved by applying annealing treatment after ECAP [10]. This application will create a process of recrystallization of the crystal structure so that in can make the structure more homogeneous [10].

By using the post-ECAP annealing principle [10], of course hypothetically there are also changes in crystal structure and texture during the ECAP process and post-ECAP annealing. For this reason, this research was conducted with the aim of proving it on Al-5052 rod. Indicators of changes in crystal structure and texture during the post-ECAP annealing process can be observed by characterization using x-ray diffraction (XRD) and electron backscatter diffraction (EBSD) techniques [10,11], both of which are also used in this study.

## 2. METHODS

Four samples used were uniform i.e. Al-5052 rods with diameter of 13.5 mm and length of 65 mm. These Al-5052 alloys have a composition of elements as shown in Tabel 1.

**Table 1.** The composition of Al-5052 alloy sample.

| Element | Composition (wt.%) |
|---------|--------------------|
| Al | 96.6300 |
| Mg | 2.6600 |
| Fe | 0.2700 |
| Cr | 0.2300 |
| Si | 0.1300 |
| Zn | 0.0120 |
| V | 0.0070 |
| Mn | 0.0060 |
| Cu | 0.0007 |

These samples were then homogenized at a temperature of 550 $^{o}$C for 12 hours. After homogenization, these samples were given ECAP treatment with the Bc route using dies which has a tube pass with 120$^{o}$ of elbow for about four passes. Illustration of dies and ECAP route Bc can be seen in Figure 1 and Figure 2. After ECAPed, three of four samples were annealed at 100 $^{o}$C, 200 $^{o}$C and 300 $^{o}$C for about 30 minutes. The remaining sample that was not given annealing treatment was used as a sample without annealing treatment.

The four samples were then characterized by Rigaku SmartLab x-ray diffractometer (XRD) with Cu-Kα tube ($\lambda$ = 1.541862 Å) to observe the crystal structure and Oxford Electron Backscatter Diffraction (EBSD) instrument for texture observation.

## 3. RESULTS AND DISCUSSION

### 3.1. XRD Analysis

Al-5052 sample is an aluminum based alloy which has a face-centered cubic (FCC) crystal structure [12]. Therefore, to observe the crystal structure of Al-5052 alloy rod which was treated with ECAP and post-ECAP annealing, an FCC investigation was performed. The results of FCC analysis on samples that have undergone the ECAP and post-ECAP annealing treatments can be seen in Table 2, Table 3, Table 4 and Table 5.

All four samples treated with ECAP route Bc have the same planes i.e. (111), (200), (220), (311), (222) and (400) (see Table 2, Table 3, Table 4 and Table 5). The planes that were identified have identical characteristics where all of *h*, *k* and *l* are odd or even. The characteristics of such planes indicate that the structure formed is FCC [13].

In each of the last columns in Table 2, Table 3, Table 4 and Table 5, there are lattice parameter calculation results at each diffraction peak. The lattice parameter values of a certainly have different variations due to different points of view in their calculations due to different planes (*hkl*). However, the actual lattice parameter values can be accurately calculated by precise lattice parameter analysis ($a_o$) using the Nelson-Riley calculation method [14]. The results of calculations using the Nelson-Riley method on these four samples can be seen in Figure 3.
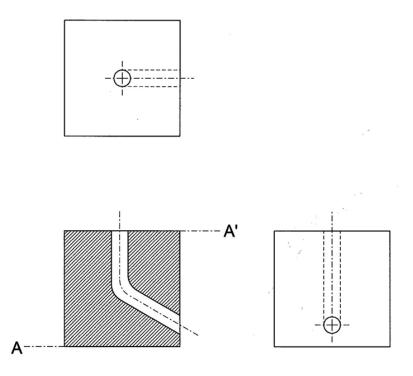
**Figure 1.** The illustration of ECAP dies with 120º of elbow of tube channel.
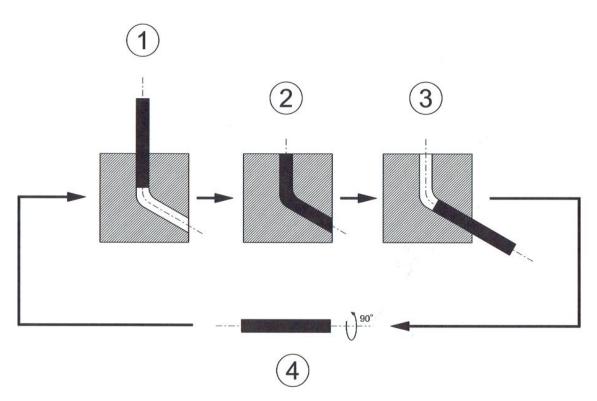


**Figure 2.** The illustration of ECAP process with Bc route.

The value of the precise lattice parameter ($a_o$) in calculations with the Nelson-Riley method is the intersection point between the linear regression lines with the y-axis (or the a-lattice parameter axis) [13,14]. The regression lines are formed by the constituent planes of the FCC structure (see Figure 3). Statistically, linear regression lines are considered to exist if they have relevant $R^2$ values [15]. Ideally, the relevant $R^2$ value is one, which means it shows a 100% correlation between $x$-axis and $y$-axes [15]. However, in real conditions it is rare to find the condition $R^2 = 1$. Therefore, in this case, the recommended $R^2$ value is $0.9 \leq R^2 \leq 1$. The FCC planes that form part of the linear regression line compilers indicate that these planes are part of the same FCC unit-cell.

Now, let us consider Figure 3.b, Figure 3.c and Figure 3.d. The six FCC planes i.e. (111), (200), (220), (311), (222) and (400) form one line of linear regression. This shows that the six planes are part of the same FCC unit-cell. This show that the FCC structure formed in the Al-5052 samples treated with ECAP and followed by annealing process of 100-300 °C has one homogeneous unit-cell and the same precise lattice parameter values. Then now let us look at Figure 3.a. In Figure 3.a it appears that there are two linear regression lines and also two planes that do not form a linear regression line i.e. (222) and (400). The two linear regression lines formed have different $a_o$ values, 4.073563 Å and 4.066668 Å. In addition, the two planes which do not form a linear regression line each have a lattice parameter value of 4.04806 Å and 4.05476 Å (see Table 2). Thus, there are four variations of lattice parameters in Figure 3.a which also indicate the existence of four variations of FCC unit-cell in samples treated

with ECAP without annealing. From the facts of this calculation result shows that there is a transformation from four FCC unit-cells that vary their lattice parameters before annealing process into uniform unit-cells with only one variation of unit-cell with a single lattice parameter. This certainly shows that the post-ECAP annealing process can tidy up the FCC structure on Al-5052 to become more homogeneous.

## 3.2. Texture Analysis

Texture analysis used was microtexture analysis using EBSD technique with representation in the form of pole figures [16,17]. The results of the pole figure representation for the FCC structure on the four samples themselves can be seen in Figure 4.

The pole figure representation in Figure 4 shows that the higher annealing temperature after ECAP will result in the texture of the FCC structure on Al-5052 becoming more random. This shows that as a result of the post-ECAP annealing treatment, even though the FCC unit-cells that are formed become more homogeneous on their lattice parameters, the orientation direction is even more varied.

The unit-cell homogeneity of the FCC structure and the random rate of orientation will certainly have implications for its mechanical properties. Therefore, the prospect of further research to see the effect of increasing unit-cell homogeneity and the randomness of orientation due to annealing after ECAP on Al-5052 rod in the future will certainly be interesting to study further.

**Table 2.** FCC investigation of ECAPed sample without post-ECAP annealing.

| $2\theta$ (deg.) | $\text{Sin}^2\theta$ | $(\text{Sin}^2\theta)/3$ | $(\text{Sin}^2\theta)/4$ | $(\text{Sin}^2\theta)/8$ | $(\text{Sin}^2\theta)/11$ | $(\text{Sin}^2\theta)/12$ | $(\text{Sin}^2\theta)/16$ | $hkl$ | $a$ (Å) |
|---|---|---|---|---|---|---|---|---|---|
| 38.440 | 0.10837 | **_0.03612_** | 0.02709 | 0.01355 | 0.00985 | 0.00903 | 0.00677 | 111 | 4.05622 |
| 44.653 | 0.14431 | 0.04810 | **_0.03608_** | 0.01804 | 0.01312 | 0.01203 | 0.00902 | 200 | 4.05877 |
| 64.876 | 0.28771 | 0.09590 | 0.07193 | **_0.03596_** | 0.02616 | 0.02398 | 0.01798 | 220 | 4.06521 |
| 77.997 | 0.39602 | 0.13201 | 0.09901 | 0.04950 | **_0.03600_** | 0.03300 | 0.02475 | 311 | 4.06307 |
| 82.557 | 0.43523 | 0.14508 | 0.10881 | 0.05440 | 0.03957 | **_0.03627_** | 0.02720 | 222 | 4.04806 |
| 99.020 | 0.57839 | 0.19280 | 0.14460 | 0.07230 | 0.05258 | 0.04820 | **_0.03615_** | 400 | 4.05476 |

**Table 3.** FCC investigation of ECAPed sample after post-ECAP annealing at 100 ℃.

| $2\theta$ (deg.) | $\sin^2\theta$ | $(\sin^2\theta)/3$ | $(\sin^2\theta)/4$ | $(\sin^2\theta)/8$ | $(\sin^2\theta)/11$ | $(\sin^2\theta)/12$ | $(\sin^2\theta)/16$ | $hkl$ | $a$ (Å) |
|---|---|---|---|---|---|---|---|---|---|
| 38.721 | 0.10990 | **_0.03663_** | 0.02748 | 0.01374 | 0.00999 | 0.00916 | 0.00687 | 111 | 4.02790 |
| 44.964 | 0.14623 | 0.04874 | **_0.03656_** | 0.01828 | 0.01329 | 0.01219 | 0.00914 | 200 | 4.03214 |
| 65.277 | 0.29088 | 0.09696 | 0.07272 | **_0.03636_** | 0.02644 | 0.02424 | 0.01818 | 220 | 4.04297 |
| 78.286 | 0.39849 | 0.13283 | 0.09962 | 0.04981 | **_0.03623_** | 0.03321 | 0.02491 | 311 | 4.05047 |
| 82.463 | 0.43442 | 0.14481 | 0.10860 | 0.05430 | 0.03949 | **_0.03620_** | 0.02715 | 222 | 4.05185 |
| 99.040 | 0.57856 | 0.19285 | 0.14464 | 0.07232 | 0.05260 | 0.04821 | **_0.03616_** | 400 | 4.05416 |

**Table 4.** FCC investigation of ECAPed sample after post-ECAP annealing at 200 ℃.

| $2\theta$ (deg.) | $\sin^2\theta$ | $(\sin^2\theta)/3$ | $(\sin^2\theta)/4$ | $(\sin^2\theta)/8$ | $(\sin^2\theta)/11$ | $(\sin^2\theta)/12$ | $(\sin^2\theta)/16$ | $hkl$ | $a$ (Å) |
|---|---|---|---|---|---|---|---|---|---|
| 38.639 | 0.10945 | **_0.03648_** | 0.02736 | 0.01368 | 0.00995 | 0.00912 | 0.00684 | 111 | 4.03612 |
| 44.861 | 0.14559 | 0.04853 | **_0.03640_** | 0.01820 | 0.01324 | 0.01213 | 0.00910 | 200 | 4.04092 |
| 65.129 | 0.28971 | 0.09657 | 0.07243 | **_0.03621_** | 0.02634 | 0.02414 | 0.01811 | 220 | 4.05114 |
| 78.216 | 0.39789 | 0.13263 | 0.09947 | 0.04974 | **_0.03617_** | 0.03316 | 0.02487 | 311 | 4.05351 |
| 82.405 | 0.43392 | 0.14464 | 0.10848 | 0.05424 | 0.03945 | **_0.03616_** | 0.02712 | 222 | 4.05419 |
| 98.920 | 0.57753 | 0.19251 | 0.14438 | 0.07219 | 0.05250 | 0.04813 | **_0.03610_** | 400 | 4.05779 |

**Table 5.** FCC investigation of ECAPed sample after post-ECAP annealing at 300 ℃.

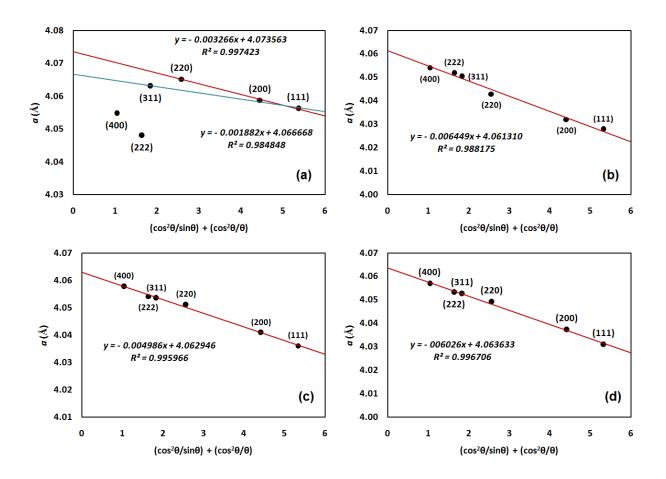| $2\theta$ (deg.) | $\sin^2\theta$ | $(\sin^2\theta)/3$ | $(\sin^2\theta)/4$ | $(\sin^2\theta)/8$ | $(\sin^2\theta)/11$ | $(\sin^2\theta)/12$ | $(\sin^2\theta)/16$ | $hkl$ | $a$ (Å) |
|---|---|---|---|---|---|---|---|---|---|
| 38.690 | 0.10973 | **_0.03658_** | 0.02743 | 0.01372 | 0.00998 | 0.00914 | 0.00686 | 111 | 4.03100 |
| 44.903 | 0.14585 | 0.04862 | **_0.03646_** | 0.01823 | 0.01326 | 0.01215 | 0.00912 | 200 | 4.03732 |
| 65.165 | 0.29000 | 0.09667 | 0.07250 | **_0.03625_** | 0.02636 | 0.02417 | 0.01813 | 220 | 4.04916 |
| 78.236 | 0.39806 | 0.13269 | 0.09952 | 0.04976 | **_0.03619_** | 0.03317 | 0.02488 | 311 | 4.05264 |
| 82.427 | 0.43411 | 0.14470 | 0.10853 | 0.05426 | 0.03946 | **_0.03618_** | 0.02713 | 222 | 4.05330 |
| 98.948 | 0.57777 | 0.19259 | 0.14444 | 0.07222 | 0.05252 | 0.04815 | **_0.03611_** | 400 | 4.05694 |

**Figure 3.** Linear regression analysis of $y = \beta_1 x + \beta_o$ (which $y$ is $a$-lattice parameter and $x$ is ($cos^2\theta/sin\theta + cos^2\theta/\theta$)) for calculating precise lattice parameter ($a_o$) using Nelson-Riley method on Bc route-ECAPed samples. (a) Without post-ECAP annealing. (b) Annealing at 100 °C. (c) Annealing at 200 °C. (d) Annealing at 300 °C.

## 4. CONCLUSION

Al-5052 rod crystal structure remains the same, both after the Bc route of ECAP process and after the post-ECAP annealing process at a temperature of 100-300 °C, where the structure is FCC.

The post-ECAP annealing process with an annealing temperature of 100-300 °C can tidy up the FCC structure of the Al-5052 rods which previously underwent ECAP treatments with Bc routes become more homogeneous which has a single FCC unit-cell with uniform lattice parameters.

However, despite an increase in the homogeneity of the FCC unit-cell after post-ECAP annealing with a temperature of 100-300 °C, the orientation of the uniform unit-cell is even more random as an additional annealing temperature after ECAP.
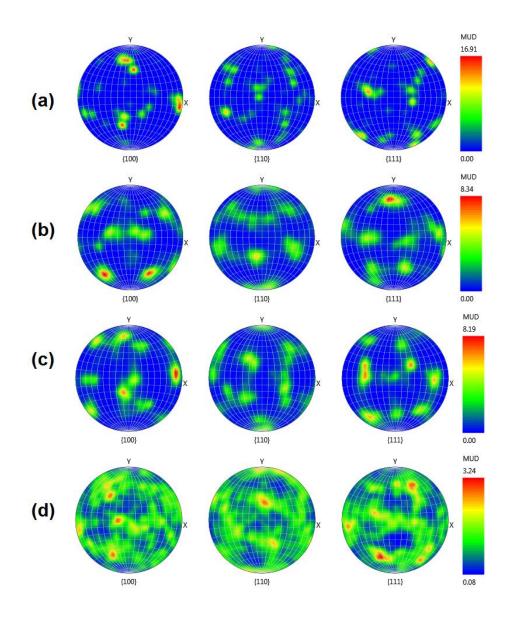
## 5. ACKNOWLEDGEMENT

**Figure 4.** Pole figure representation of FCC structure on Bc route-ECAPed Al-5052 samples. (a) Without post-ECAP annealing. (b) Annealing at 100 ºC. (c) Annealing at 200 ºC. (d) Annealing at 300 ºC.

## REFERENCES

[1]  Yogesha, K. K., Joshi, A., Jayaganthan, R. Fatigue Behavior of Ultrafine-grained 5052 Al Alloy Processed Through Different Rolling Methods. JMEPEG. 2017; 26 (6): 2826-2836.

[2]  Batmanghelich, F., Hariri, M. B., Sharifi-Asl, S., Yaghoubinezhad, Y., Mortazavi, G., Seo, Y. W. Corrosion and Time Dependent Passivation of Al 5052 in the Presence of $H_2O_2$. Met. Mater. Int. 2016; 22 (4): 609-620.

[3]  Woo, M. A., Noh, H. G., Song, W. J., Kang, B. S., Kim, J. Experimental Validation of Numerical Modeling of Electrohydraulic Forming Using an Al 5052-H34 Sheet. Int. J. Adv. Manuf. Technol. 2017; 93: 1819-1828.

[4]  Anas, N. M., Dhindaw, B. K., Zuhailawati, H., Abdullah, T. K., Anasyida, A. S. Effect of Initia Microstructure on Properties of Cryorolled Al 5052 Alloy Subjected to Different Annealing Treatment Temperatures. JMEPEG. 2018; 27: 6206-6217.

[5]  Avvari, M. Narendranath, S. Effect of Secondary $Mg_{17}Al_{12}$ Phase on AZ80 Alloy Processed by Equal Channel Angular Pressing (ECAP). Silicon. 2018; 10: 39-47.

[6]  Kumar, S. R., Gudimetla, K., Mohanlal, S., Ravisankar, B. Effect of Mechanically Alloyed Graphene-reinforced Aluminum by Equal Channel Angular Pressing. Trans. Indian Inst. Met. 2019; 72 (6): 1437-1441.

[7]  Kondaveeti, C. S., Sunkavalli, S. P., Undi, D., Kumar, L. V. H., Gudimetla, K., Ravisankar, B. Metallurgical and Mechanical Properties of Mild Steel Processed by Equal Channel Angular Pressing (ECAP). Trans. Indian Inst. Met. 2017; 70 (1): 83-87.

[8]  Derakhshandeh-Haghighi, R., Jahromi, S. A. J.. The Effect of Multi-pass Equal-channel Angular Pressing (ECAP) for Consolidation of Aluminum-Nano Alumina Composite Powder on Wear Resistance. JMEPEG. 2016; 25 (2): 687-696.

[9]  Khelfa, T., Rekik, M. A., Munoz-Balanos, J. A., Cabrera-Marrero, J. M., Khitouni, M. Microstructure and Strengthening Mechanism in an Al-Mg-Si Alloy Processed by Equal Channel Angular Pressing. Int. J. Adv. Manuf. Technol. 2018; 95: 1165-1177.

[10] Bahadori, S. R., Dehghani, K. Influence of Intermediate Annealing on the Nanostructure and Mechanical Properties of Pure Copper Processed by Equal Channel Angular Pressing and Cold Rolling. Metallurgical and Materials Transactions A. 2015; 46A: 2796-2802.

[11] Serebryany, V. N., D'yakonov, G. S., Kopylov, V. I., Salishchev, G. A., Dobatkin, S. V. Texture and Structure Contribution to Low-temperature Plasticity Enhancement of Mg-Al-Zn-Mn Alloy MA2-1hp after ECAP and Annealing. The Physics of Metals and Metallography. 2013; 114 (5): 448-456.

[12] Gafner, Y. Y., Baidyshev, V. S., Gafner, S. L. Effect of Disoreder on the Structure of Small Aluminum Clusters During Heat Treatment. Physics of the Solid State. 2015; 57 (1): 188-196.

[13] Suryanarayana, C. and Grant Norton. 1998. M. *X-ray Diffraction: a Practical Approach*. New York, New York: Plenum Press.

[14] Nelson, J. B., Riley, D. P. An Experimental Investigation of Extrapolation Methods in the Derivation of Accurate Unit-cell Dimensions of Crystals. Proc. Phys. Soc. 1945; 57: 160-177.

[15] Weisberg, S. 2005. *Applied Linear Regression,* 3$^{rd}$ Ed. Hoboken, New Jersey: John Wiley & Sons, Inc.

[16] Engler, O. and Randle, V. 2010. *Introduction to Texture Analysis: Macrotexture, Microtexture and Orientation Mapping*. Boca Raton, Florida: CRC Press, Taylor and Francis Group.

[17] Suwas, S. and Ray, R. K. 2014. *Crystallographic Texture of Materials*. London: Springer-Verlag.